ADVANCED MATERIALS

ASSEMBLY

Holographically shaped light fields can be employed to create highly ordered structures of various kinds of microscopic and nanoscopic particles. M. Woerdemann and co-workers demonstrate on page 5199 an optical-tweezers assembly-line that utilizes such light fields in combination with microfluidics and colloidal interactions to construct complex and functional assemblies of Zeolite L crystals, which exhibit exciting photonic properties.

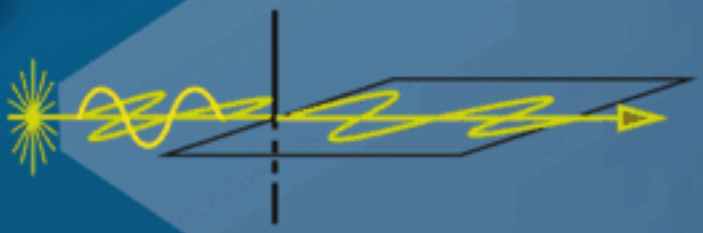

WILEY-VCH

Optical-Tweezers Assembly-Line for the Construction of Complex Functional Zeolite L Structures

M. Veiga-Gutiérrez, M. Woerdemann, E. Prasetyanto, C. Denz, and L. De Cola*

Supramolecular assembly of molecules is a concept extensively exploited in chemistry to obtain functionalities and structures not achievable by synthetic strategies based on covalent bonds.[1,2] Recently, attention has shifted from molecules to nano- and micro-objects,[3] such as (gold) particles,[4] rods,[5,6] and plates[7] with the aim to assemble them in analogy to what has been done with molecules. Porous microsized crystals such as zeolites are particularly interesting as building blocks since, by accommodating small molecules within their nanopores, they are able to bridge the gap between the micro- and nanoworlds.[8–12] The pore structure of zeolite L consists of one-dimensional channels running across the whole crystal axis.[12] If loaded with organic dyes, the confinement exerted by the pore dimensions enhances the emissive properties of the molecular guests, leading to materials that can be used as effective light harvesting antenna systems,[8] luminescent labels for imaging,[13,14] or for bio-medical applications,[15] to mention a few. In turn, the crystals themselves may also be arranged on a larger scale, extending the ordering from the molecular to the macroscopic scale and leading to materials with exciting properties such as mono-directional transfer of electronic excitation energy, or coherent emission of stimulated radiation.[16–18] However, the fine control over each individual crystal remains a difficult task, and most methods available for assembling zeolite L crystals are limited to surface functionalization and subsequent reaction in solution.[6,19,20] Nevertheless recently, we have demonstrated that using *holographic optical tweezers* (HOT)[21,22] this challenge can be elegantly addressed.[23]

Optical tweezers employ a tightly focused laser beam which can transfer momentum to transparent microparticles and hence confine them near the focal spot.[24] Utilizing holographically tailored laser light fields, multiple optical traps can be used simultaneously to gain full control over several individual zeolite crystals, thus opening the possibility for the assembly of complex and defined structures.[23] The aim of this work is therefore to develop a simple and robust method based on HOT which will lead to the formation of complex and functional assemblies of zeolites.

Dr. M. Woerdemann, Prof. C. Denz
Institut für Angewandte Physik
Westfälische Wilhelms-Universität Münster
Corrensstraße 2, 48149 Münster, Germany
E-mail: woerde@uni-muenster.de
Dr. M. Veiga-Gutiérrez, Dr. E. Prasetyanto, Prof. L. De Cola
Physikalisches Institut and Center for Nanotechnologie
Heisenbergstraße 11, 48149 Münster, Germany

DOI: 10.1002/adma.201201946

As proof of principle, we have created several assemblies based on zeolite L. We have used long cylindrical zeolites with average length and diameter of 4 μm × 2 μm or 2 μm × 1 μm. The strong asymmetry of the crystals makes it easy to monitor the success of the manipulation and the orientation. For some of those structures, we take advantage of luminescent dyes that can act as guests, leading to structures with photonic functionalities: a two-color monolayer, and a structure which demonstrates spatially selective switching of light emission patterns and furthermore can serve as a microsized sensor for light polarization. For the two-color monolayer, the building blocks have been loaded either with red emissive Oxazine 1 or yellow emissive DXP. These dyes have been chosen since they present good quantum yields, are easily inserted, and can be selectively excited by using conventional dichroic filters. Both dyes align within the zeolite channels. While dyes with structure similar to Oxazine 1 have been reported to tilt within the cavity, DXP aligns strictly parallel to the channels and hence to the axis of the crystal.[25] Its electronic transition dipole moment (ETDM) coincides for absorption and emission and it is parallel to the molecular major axis. As a result, the whole crystal also emits light in an anisotropic way.[11] Thus, in a structure with crystals having defined orientations with respect to a polarized external excitation source, only those presenting a favorable orientation will be able to absorb, and consequently emit light.[25,26]

The currently available methods to pattern zeolites on surfaces or assemble them in rod-like structures rely on chemical functionalization or physisorption of the bulk material.[6,19] Covalent functionalization is particularly advantageous, since it leads to permanent structures. Nevertheless, this type of functionalization, and especially the selective modification of the channel entrances,[27] requires a complex multistep synthetic approach.

On the other hand, assemblies of particles can also be created on the basis of colloidal interactions.[28–30] Zeolite L crystals are aluminosilicates that present a net negative charge at their surface, compensated by the presence of cations within their structure. As a result, in neutral conditions, the repulsion exerted by their ionic double layers keeps them stable in solution. However, in a medium of high ionic strength, the ionic double layers are screened and zeolites can come in close contact. In this instance, Van-der-Waals forces dominate and zeolites adhere effectively to each other or to glass surfaces.[31] These forces, although classified as weak, are stronger than the force typically exerted by the optical tweezers, and also strong enough to keep zeolites fixed in conditions of moderate fluid flow. In order to create permanent assemblies, the pH value can be tuned. The rate of hydrolysis of the silica bonds is described by a curve with a minimum at pH 7, increasing at acidic or basic pH.[32] The rate of condensation of silanol groups has a

maximum between pH 7 and 8, with a steep decrease at basic or acidic pH.[33] Therefore the goal is to hydrolyze the glass surface and to promote condensation between the silanol groups of the glass surface and the zeolites in order to immobilize them permanently on the substrate. We have chosen to work at pH 8.5, the crossing point of both curves, using an ammonia-based buffer. The reaction, despite being slow, has been proven to be very robust. Silica particles immobilized by this method can no longer be separated after 48 h.[28]

In order to reduce uncontrolled adsorption of the zeolites on the glass, the use of anionic surfactants is a winning strategy. Above the critical micellar concentration, the surfactant surrounds the zeolites preventing close contact with the glass surface or with each other.[34,35] As a consequence, the zeolites exhibit strong Brownian motion in the presence of anionic surfactants even after being in contact with a glass substrate for more than 12 h. Taking into account the above discussed observations, our approach consists in providing a surfactant-rich (non-sticking) environment to optimize the supply, control and manipulation of the building blocks, and another salt-rich (sticking) environment where the assembly can be constructed. To handle both inputs and control them in a spatial and temporal way we performed the assemblies within a microfluidic channel. The microfluidic platform therefore plays two important roles: first, it provides a constant flow of building blocks and second, it sets the chemical conditions to ensure permanent assemblies. We created a Y-shaped PDMS microchannel (height 50 µm, width of the small arms 300 µm, width of the big arm 1 mm), where the first arm is supplied with a surfactant-rich solution of zeolites (sulfonic acids mixture, see experimental section), and the second arm with a highly concentrated solution of NaCl (0.5 M). Both channels are pumped with independent microfluidic pumps at the same flow rate (6.94 nl/s). At the position where the two arms merge, a laminar flow (Reynolds number Re < 1) establishes which separates the two phases. The assembly process is carried out in several steps: i) identification of suitable building blocks in the surfactant phase, ii) trapping of the individual target crystals with the optical tweezers, iii) transfer to the construction site, iv) orientation of the particles in the desired position, v) deposition at the target contact surface and iv) exchange of the salt-rich solution for a pH 8.5 solution once the whole structure is finished. The process resembles an "assembly line" on the micrometer scale and has a high potential for automation of several or all of the steps.

As first test of the optical-tweezers assembly-line (OTAL), we created a monolayer of 34 standing zeolites, describing the acronym of our university ("W.W.U.", **Figure 1**). The configuration was constructed using a single optical trap in which the major axis of the crystals always aligns parallel to the optical axis of the light beam. When placing each zeolite at the contact surface, it becomes instantly immobilized (by the van-der-Waals forces), resulting in a pattern of upright zeolites.

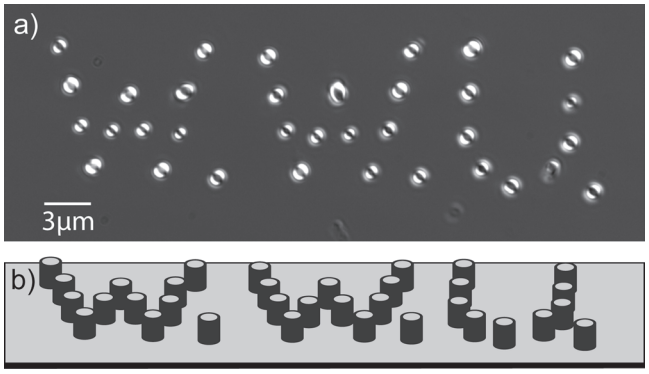

Figure 1. a) Monolayer of vertically standing zeolites (DIC image) on a glass surface describing the acronym W.W.U. (Westfälische Wilhelms-Universität). b) 3D sketch of the configuration.

Increasing the complexity, a second structure is created containing dye-loaded zeolites which are assembled following a color order. **Figure 2** shows a two-color monolayer of upright zeolites observed under different illumination conditions. The rows are formed by zeolites filled with the yellow-emitting DXP dye or with the red-emitting Oxazine 1 molecules. Using green excitation light (λ_{Ex} = 531 ± 20 nm), selective excitation of the DXP loaded zeolites is achieved and the yellow emission (λ_{Em} = 593 ± 20 nm) is observed. Switching the excitation to red light (λ_{Ex} = 630 ± 30 nm) results in red emission (λ_{Em} = 690 ± 20 nm) of the selectively excited Oxazine 1 loaded zeolites. Therefore, the luminescence pattern can easily be switched between different states addressing only the desired pattern.

Both former structures (Figure 1 and 2), are formed by zeolites standing upright on a substrate and can be achieved using

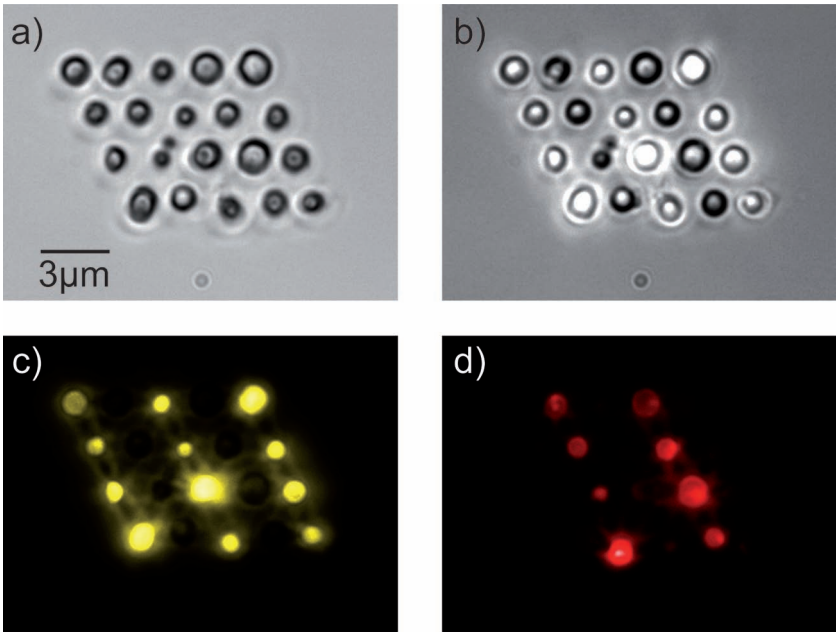

Figure 2. Monolayer of vertically standing zeolites on the glass surface. a) Bright-field illumination. b) Bright-field and simultaneous fluorescence excitation. c) Excitation through green band-pass filter. d) Excitation through red band-pass filter.

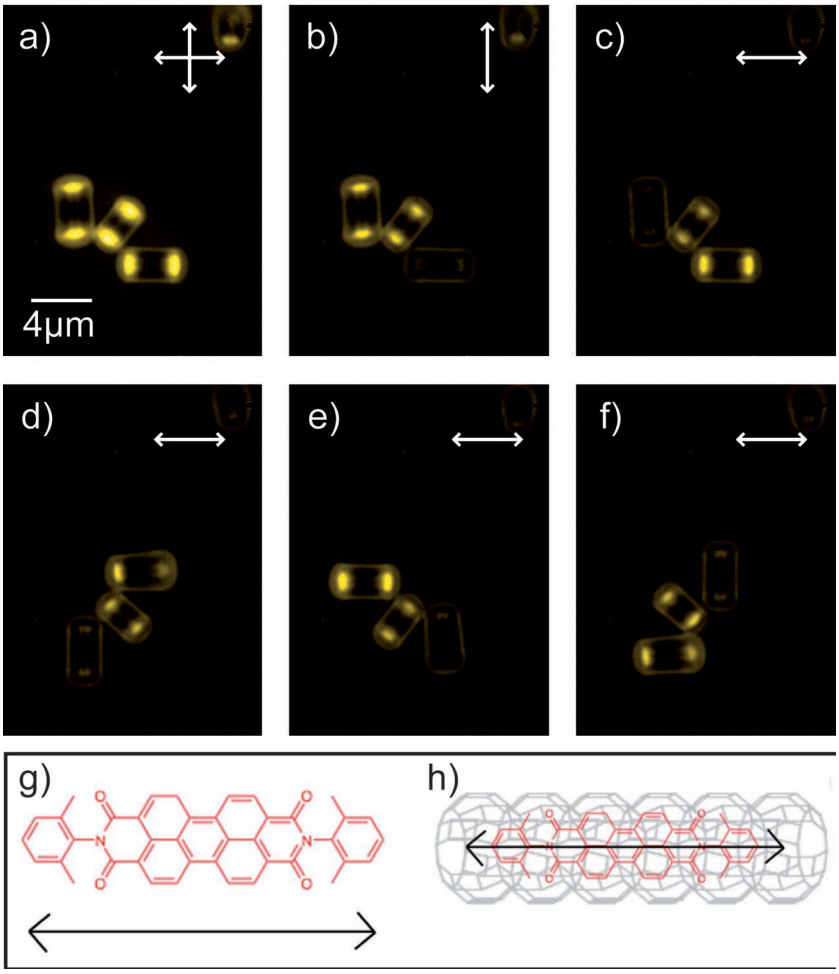

Figure 3. a–f) Dynamic structure of zeolites hold together by HOT (see also supporting video): a) non-polarized excitation; b) vertically polarized excitation; c–f) horizontally polarized excitation; g) DXP chemical structure and direction of its ETDM. The molecule is symmetrical and hence ETDM becomes bidirectional; h) alignment of DXP within a zeolite L and resulting ETDM of the whole crystal.

conventional (single beam) optical tweezers. The elongation of a zeolite leads to an orientation, where only the top or bottom of the cylinders can be observed through the microscope. Hence, the crystals are automatically aligned in the optimal orientation for the upright deposition on the substrate. More complex structures, for which the full control of the crystals is necessary, can only be achieved by HOT.[23] The most effective way to tilt the zeolite particles is by the use of one or multiple additional traps, and to place these traps at the edges of the crystal.[23,36] **Figure 3** shows a dynamic (non-permanent) structure of three DXP-loaded zeolites held by six optical traps. The DXP molecules, along these very long zeolites, are mostly diffused in the first micrometer of the crystals and therefore their emission is detected at each edge of the zeolites. Having oriented the zeolites so that their major axes point along the transverse plane of observation, Figure 3a–f show that the emission is anisotropic due to the perfect orientation of the dyes in the narrow channels (see Figure 3g,h).[25] Therefore, the illumination is changed from non-polarized (a), to vertical polarized (b), to horizontal polarized (c). From (b) and (c), it is clearly seen that structures being perpendicularly oriented with respect to the excitation axis of the incident polarized light do not absorb light and hence do not fluoresce.[25–26,37] In the second row (d–f), the polarization is kept horizontal and the whole assembly is rotated by 90° each time. In this case, the luminescent properties of the assembly are dependent on its rotation position.

This result has motivated the concept of a permanent structure serving as polarization sensor, as shown in **Figure 4**. The structure consists of 10 equally spaced zeolites lying on the circumference of a circle and having their long axes oriented at angles of 10° with respect to each other. There is an additional zeolite which is placed upright on the surface, and which serves as reference at the center of the circle. Figure 4a and 4b are taken under bright-field and non-polarized fluorescence excitation conditions, respectively. With the non-polarized excitation, the whole assembly exhibits fluorescence (Figure 4b).

In this structure, DXP loading is more homogeneous than for the samples shown in Figure 3, and fluorescence is seen along the whole crystals for some of them. This reveals one of the advantages of the OTAL, which enabled us to select the best candidates as building blocks. Figure 4c is taken in conditions of horizontal excitation. Zeolites oriented perpendicularly with respect to the excitation axis do not exhibit fluorescence, whereas as the angle between the zeolite's axis and the excitation axis decreases, the fluorescence intensity increases. In Figure 4d, polarization is changed to vertical and, as expected, an analogous behavior but in the opposite direction is observed. In order to quantify the photonic response of the structure, the light intensity of each zeolite was measured with a calibrated detection camera and normalized by the intensity values of the zeolites under unpolarized light. In Figure 4e and 4f, the normalized emission intensity is plotted versus the angle of orientation. According to Malus' law, the dependence is expected to be of a cosine square type in the case of perfectly polarized light and perfect (narrow) polarization response of the zeolites.[26] A best fitted cosine-square curve is shown with the data, revealing evidently a complete agreement.

Interestingly, the zeolite placed as reference at the center of the circle also exhibits fluorescence. The reason for this response is not obvious because the zeolite's channels are aligned parallel to the direction of the fluorescence illumination, and thus perpendicular with respect to any transverse electric field vector. The cosine-square dependence indicates that dye molecules which are strictly perpendicular oriented with respect to the electric field vector of the excitation light will not be excited.[26] In strong focusing conditions–like in this case

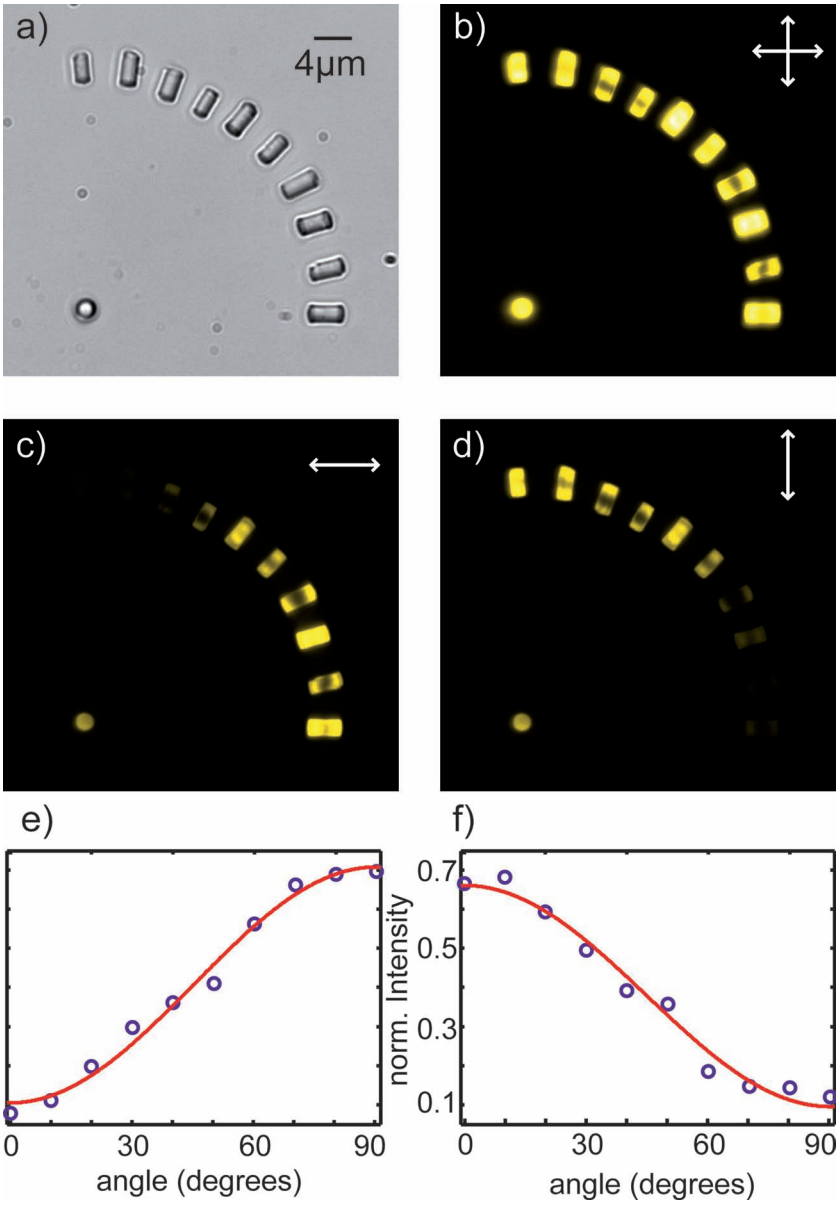

Figure 4. a–d) Permanent structure of 11 zeolites on glass surface: a) bright-field illumination; b) non-polarized excitation; c) horizontal polarization; d) vertical polarization; e) intensity vs. angle using horizontal excitation; f) intensity vs. angle using vertical excitation.

where an NA = 1.49 microscope objective is used to achieve epifluorescence illumination–, however, the electric field vector can have a significant axial component.[38] This axial component is parallel to the channels of the upright zeolite crystal and thus the dye molecules, and apparently causes the fluorescence response.

Finally, our approach also enables the construction of 3D structures as shown in **Figure 5**, opening the possibility of constructing, for example, photonic band-gap materials.[28,30,39] A "tower" of six zeolite L crystals built on a glass substrate is presented. Each layer consists of two parallel-oriented crystals; the structure consists of three layers. The diameter of the crystals is consistent with the measured layer-layer distance of approximately 2 μm. The second and third layers are blurry since they are observed from underneath with an inverted microscope through the other layers which distort the image.

Similar approaches have also previously taken advantage of optical tweezers and colloidal interactions to assemble simple micro-sized particles.[29] Alternatively, particles have also been fixed by polymerization of the surrounding medium after trapping them in the desired configurations.[39,40] Benito et al.[28] made use of depletion interactions in order to construct 3D structures based on polystyrene microspheres. They connected through a 1 mm gap two regions of a microscope slide, one containing a stable suspension of microspheres in water while the other contained viscous poly(sodium 4-styrenesulfonate). In that work, the limiting factors were the long transfer times between the two regions and the limited supply of building blocks. Both problems are circumvented with the OTAL. Whereas the continuous supply is ensured by the microfluidic flow, the transfer from the supply to the construction site takes less than 20 seconds even in the current implementation which is not yet optimized for maximum processing speed. In our case, the limiting step is the tilting of the zeolites before assembly. To achieve this without disturbances by the fluid flow, the flow was usually stopped while tilting. As soon as the zeolites are placed in the target position with the desired orientation, the flow is reinitiated to avoid mixing of the two phases.

In conclusion we have presented a simple, robust, and versatile method for the construction of permanent and functional 2D and 3D microstructures of zeolites, or other silica based particles, by combining HOT,

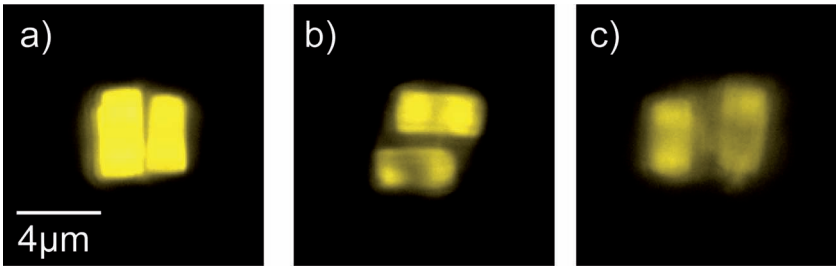

Figure 5. 3D "tower" consisting of 6 zeolite crystals: a) at the surface; b) 2.1 μm over the surface; c) 4.2 μm over the surface.

microfluidics, and colloidal interactions. The OTAL has a high potential for automation: optimization of the microfluidics could lead to the use of several "lines" in parallel, each of them with different building blocks; optimization of the optics would allow performing multiple operations in parallel. This would improve operation speed and eventually can lead to the production scale of customized microstructures, finding potential applications in microelectronics, photonics, biomedicine or sensing technology. Colloidal interactions could be combined with chemical functionalization so as to expand the methodology to organic materials.

The demonstrated structures give an idea of possible functionalities. We have shown 2D and 3D structures of different geometrical complexity, hybrid assemblies of differently loaded zeolites, and light-induced selective switching of microscopic illumination patterns. The sophisticated arrangement of zeolites loaded with polarization-sensitive dyes suggests exciting applications as micro polarization-sensors or for the characterization of the polarization properties of new dyes.

Experimental Section

Chemicals: *N*,*N*-bis(2,6-dimethylphenyl)-3,4:9,10-perylentetracarboxylic diimide (DXP) was purchased from Aldrich and Oxazine 1 from Molecular Probes. The cylindrical zeolite L crystals were prepared according to a procedure described in the literature.[25] Crystals loaded with DXP and Oxazine 1 were prepared by gas-phase insertion and ion exchange, respectively.[25]

As surfactant, we used a 10% aqueous solution of the commercial wetting agent Agepon (Agfa), which is an aqueous mixture of laurylpolyglycoether, with n-alkyl (C10–18) sulfonic acids sodium salts and benzoic acid sodium salt. The surfactant only had the role of avoiding unwanted adherence of the zeolites; other anionic surfactants could be used.

Optical-Tweezers Workstation: We employed a holographic optical tweezers (HOT) system that was self-developed and integrated into a commercially available Nikon Ti inverted microscope. The microscope was equipped with fluorescence illumination, and motorized focus control and translation stage. The HOT system enabled the dynamic and interactive generation of single and multiple optical tweezers that could be steered independently and positioned freely within the field of view. The manipulated particles were observed with bright-field illumination, fluorescence illumination, or differential interference contrast (DIC), respectively. Details of the HOT system can be found in previous publications.[23,36]

Microfluidic Platform: The microfluidic setup consisted of a custom-made PDMS Y-channel that was served by two computer-controlled high-precision syringe pumps (PSD/3 mini from Duratec, Germany). For the actual experiments, we used the minimal flow rate possible with the employed syringes (25 µl each) of 6.94 nl/s from each pump. Between different experiments, the channels were flushed with higher flow rates of up to 2.5 µl/s per pump.

PDMS Y-Channel Preparation: The PDMS channels were prepared from polytetrafluoroethylene-coated silicon relief masters, which were initially embedded in a custom-made casting mold. The PDMS (Sylgart 184 from Dow Corning) was degassed for 30 min in a vacuum desiccator and poured into the mold. After baking, the bottom of the casting mold together with the silicon master was removed. The PDMS surface and a clean microscopy cover glass were exposed to ozone for 15 min and then assembled immediately. As a result, the cover glass was permanently glued to the PDMS and serves as the bottom of the microfluidic channel.

Image Acquisition and Processing: Microscopy images were acquired using an intensity-calibrated monochrome 10bit CCD camera. Quantitative data were extracted directly from the raw images while the images shown were optimized for visibility using standard contrast filters. Furthermore, color (yellow/red) was applied to some of the images, in order to reproduce the original colors that were selected by fluorescence filters but not maintained by the monochrome camera.

Acknowledgements

This work was supported by the Deutsche Forschungsgemeinschaft in the frame of the German-Chinese TRR61. L.D.C. and M.V.G. thank ERA NanoSci programme (DFG: DE 1523). Christina Alpmann and André Devaux are greatly acknowledged for helpful discussions. We thank Michael Esseling and Stefan Gläsener for assisting in the development of the microfluidic platform.

Received: May 15, 2012
Published online: July 16, 2012

[1] Nadrian C. Seeman, Angela M. Belcher, *Proc. Natl. Acad. Sci. USA* **2002**, *99*, 6451.
[2] P. Andres, U. Schubert, *Adv. Mater.* **2004**, *16*, 1043.
[3] K. B. Yoon, *Acc. Chem. Res.* **2007**, *40*, 29.
[4] M. Daniel, D. Astruc, *Chem. Rev.* **2004**, *104*, 293.
[5] S. Hurst, E. Payne, L. Qin, C. Mirkin, *Angew. Chem. Int. Ed.* **2006**, *45*, 2672.
[6] B. Schulte, M. Tsotsalas, M. Becker, A. Studer, L. De Cola, *Angew. Chem. Int. Ed.* **2010**, *49*, 6881.
[7] T. Clark, J. Tien, D. Duffy, K. Paul, G. Whitesides, *J. Am. Chem. Soc.* **2001**, *123*, 7677
[8] G. Calzaferri, K. Lutkouskaya, *Photochem. Photobiol. Sci.* **2008**, *7*, 879.
[9] G. Calzaferri, A. Devaux, in *Supramolecular Effects in Photochemical and Photophysical Processes*, (Eds. V. Ramamurthy, Y. Inoue), John Wiley & Sons, Inc., Hoboken, NJ, USA **2010**.
[10] A. Devaux, F. Cucinotta, S. Kehr, L. De Cola, in *Functional Supramolecular Architectures: for Organic Electronics and Nanotechnology*, (Eds. P. Samori, F. Cacialli) Wiley-VCH, Weinheim, Germany **2010**.
[11] M. Busby, A. Devaux, C. Blum, V. Subramaniam, G. Calzaferri, L. De Cola, *J. Phys. Chem. C* **2011**, *115*, 5974.
[12] a) D. Bruhwiler, G. Calzaferri, *Microporous Mesoporous Mater.* **2004**, *72*, 1; b) G. Calzaferri, *Langmuir* **2012**, *28*, 6216.
[13] M. Tsotsalas, M. Busby, E. Gianolio, S. Aime, L. De Cola, *Chem. Mater.* **2008**, *20*, 5888.
[14] M. M. Tsotsalas, K. Kopka, G. Luppi, S. Wagner, M. P. Law, M. Schafers, L. De Cola, *ACS Nano* **2010**, *4*, 342
[15] C. A. Strassert, M. Otter, R. Q. Albuquerque, A. Hone, Y. Vida, B. Maier, L. De Cola, *Angew. Chem. Int. Ed.* **2009**, *48*, 7928.
[16] A. Ruiz, H. Li, G. Calzaferri, *Angew. Chem. Int. Ed.* **2006**, *45*, 5282.
[17] P. Cao, Y. Wang, H. Li, X. Yu, *J. Mater. Chem.* **2011**, *21*, 2709.
[18] G. Calzaferri, A. Zabala, H. Li, S. Huber, *Patent application WO 2007/012216*, **2005**.
[19] K. Ha, Y.-J. Lee, D.-Y. Jung, J. H. Lee, K. B. Yoon, *Adv. Mater.* **2000**, *12*, 1614
[20] H. R. Li, Y. G. Wang, W. J. Zhang, B. Y. Liu, G. Calzaferri, *Chem. Commun.* **2007**, 2853
[21] M. Reicherter, T. Haist, E. Wagemann, H. Tiziani, *Opt. Lett.* **1999**, *24*, 608
[22] J. Curtis, B. Koss, D. Grier, *Opt. Commun.* **2002**, *207*, 169
[23] M. Woerdemann, S. Gläsener, F. Hörner, A. Devaux, L. De Cola, C. Denz, *Adv. Mater.* **2010**, *22*, 4176
[24] A. Ashkin, J. Dziedzic, J. Bjorkholm, S. Chu, *Opt. Lett.* **1986**, *11*, 288
[25] G. Calzaferri, S. Huber, H. Maas, C. Minkowski, *Angew. Chem. Int. Ed.* **2003**, *42*, 3732
[26] S. Megelski, A. Lieb, M. Pauchard, A. Drechsler, S. Glaus, C. Debus, A. Meixner, G. Calzaferri, *J. Phys. Chem. B* **2001**, *105*, 25

[27] S. Huber, G. Calzaferri, *Angew. Chem. Int. Ed.* **2004**, *43*, 6738
[28] D. Benito, D. Carberry, S. Simpson, G. Gibson, M. Padgett, J. Rarity, M. Miles, S. Hanna, *Opt. Express* **2008**, *16*, 13005
[29] D. Erenso, A. Shulman, J. Curtis, S. Elrod, *J. Mod. Opt.* **2007**, *54*, 1529
[30] H. Deng, G. Li, H. Liu, Q. Dai, L. Wu, S. Lan, A. Venu Gopal, V. Trofimov, T. Lysak, *Opt. Express* **2012**, *20*, 9616
[31] J. Israelachvili, *Intramolecular and Surface Forces*, 3rd edition, Academic Press, San Diego, CA, USA **2011**, Ch. 14.
[32] C. Brinker, *J. Non-Cryst. Solids* **1988**, *100*, 31
[33] R. Iler. *The Chemistry of Silica: Solubility, Polymerization, Colloid and Surface Properties and Biochemistry of Silica*, John Wiley & Sons, Hoboken, NJ, USA **1979**, Ch. 3.
[34] N. Filipovic-Vincekovic, L. Sekovanic, D. Zitnik, *Powder Technol.* **1980**, *27*, 251
[35] Y. Zhang, Y. Shen, C. Jin, Y. Cao, W. Gao, L. Cui, *Mater. Res. Bull.* **2010**, *45*, 651
[36] F. Hörner, M. Woerdemann, S. Müller, B. Maier, C. Denz, *J. Biophoton.* **2010**, *3*, 468
[37] H. Maas, A. Khatyr, G. Calzaferri, *Microporous Mesoporous Mater.* **2003**, *65*, 233
[38] L. Novotny, B. Hecht. *Principles of Nano-optics*, Cambridge University Press, Cambridge, UK **2006**, Ch. 3.
[39] Y. Roichman, D. Grier, *Opt. Express* **2005**, *13*, 5434
[40] P. Jordan, H. Clare, L. Flendrig, J. Leach, J. Cooper, M. Padgett, *J. Mod. Opt.* **2004**, *51*, 627